remote sensing

MDPI

Article

Remote Sensing for Restoration Change Monitoring in Tropical Peat Swamp Forests in Malaysia

Chloe Brown [1], Sofie Sjögersten [2], Martha J. Ledger [3], Faizal Parish [4] and Doreen Boyd [1,*]

[1] School of Geography, University of Nottingham, Nottingham NG7 2QL, UK; chloebrown.rs@gmail.com
[2] School of Biosciences, University of Nottingham, Loughborough LE12 5RD, UK
[3] School of Biological Sciences, University of Hong Kong, Hong Kong
[4] Global Environment Centre, Petaling Jaya 47300, Selangor, Malaysia; fparish@gec.org.my
* Correspondence: doreen.boyd@nottingham.ac.uk

Abstract: Effective planning and management strategies for restoring and conserving tropical peat swamp ecosystems require accurate and timely estimates of aboveground biomass (AGB), especially when monitoring the impacts of restoration interventions. The aim of this research is to assess changes in AGB and evaluate the effectiveness of restoration efforts in the North Selangor Peat Swamp Forest (NSPSF), one of the largest remaining peat swamp forests in Peninsular Malaysia, using advanced remote sensing techniques. A Random Forest machine learning method was employed to upscale AGB estimates, derived from a 'LiDAR AGB model', to larger landscape-scale areas with Sentinel-2 spectral and textural variables. The time period under investigation (2015–2018) marked a concentrated phase of restoration and regeneration efforts in NSPSF. The results demonstrate an overall increase in tropical peat swamp AGB during these years, where the total amount of estimated AGB stored in NSPSF increased from 19.3 Tg in 2015 to an estimated 19.8 Tg in 2018. The research found that a tailored variable selection approach improved predictions of AGB, with optimised input variables (n = 62) and parameter adjustments producing a good plausible result (R^2 = 0.80; RMSE = 55.2 Mg/ha). This paper concludes by emphasizing the importance of long-term studies (>5 years) for analyzing the success of tropical peat swamp restoration methods, with a potential for integrating remote sensing technology.

Keywords: tropical peat swamp forest; restoration; aboveground biomass change detection

check for updates

Citation: Brown, C.; Sjögersten, S.; Ledger, M.J.; Parish, F.; Boyd, D. Remote Sensing for Restoration Change Monitoring in Tropical Peat Swamp Forests in Malaysia. *Remote Sens.* **2024**, *16*, 2690. https://doi.org/10.3390/rs16152690

Academic Editor: Henning Buddenbaum

Received: 22 May 2024
Revised: 9 July 2024
Accepted: 15 July 2024
Published: 23 July 2024

Copyright: © 2024 by the authors. Licensee MDPI, Basel, Switzerland. This article is an open access article distributed under the terms and conditions of the Creative Commons Attribution (CC BY) license (https://creativecommons.org/licenses/by/4.0/).

1. Introduction

Human encroachment and intensified agricultural activities have threatened the function, and even existence, of tropical peat swamp forests in Southeast Asia [1–3]. The restoration of these degraded tropical peat swamp ecosystems poses an enormous global challenge for both scientists and policymakers alike [4–6]. Tropical peatland restoration is supported by a number of both national and international goals relating to ecosystem management, climate change mitigation, and sustainable development. For example, peatland restoration is recognised as a key focus in reaching carbon emission reduction targets under the Kyoto Protocol [7] and as a terrestrial ecosystem management and protection aim under the United Nations Sustainable Development Goal number 15 (SDG 15). Therefore, there is an urgent need for the development of landscape-scale measures for verifying and quantifying restoration procedures in order to achieve the goals and commitments related to tropical peat swamp forest recovery.

Mapping aboveground biomass (AGB) dynamics and assessing their changes in response to anthropogenic activities is critical to understanding and monitoring the current status of tropical peatlands, as well as the performance of restoration practices [8–11]. The collection of AGB data has traditionally been based on forest inventory plots [12]. However, despite generating accurate results [13], these ground-based methods have been deemed

expensive, time-consuming, and often limited by their sample size and spatial distribution over landscape scales [14,15]. Advances in remote sensing technology and improved computing and image processing techniques have made it possible to estimate large-scale forest AGB in a robust, cost-effective manner [16–18]. In particular, spaceborne sensors have generated a vast archive of data at a spatial and temporal scale appropriate to support ecosystem restoration and monitoring programs [19,20]. For example, the European Space Agency's Sentinel-2 constellation, which carries the MSI sensor with improved spatial and temporal resolution over existing optical spaceborne sensors (e.g., the Landsat series) and unique spectral band selection, promises to benefit global forest AGB monitoring efforts [21,22]. Optical sensors, such as those aboard Sentinel-2, are often limited to recording the reflectance in the topmost part of a forest canopy. The restrictions of optical data in delivering detailed vertical information on forest stand structure have directly impacted the accuracy of forest AGB assessment [23]. Despite this shortcoming, spaceborne optical imagery remains a popular data option in large-scale forestry applications due to the wide availability of data sources, access to archival datasets, and low cost (at times with no acquisition cost).

Aside from optical remote sensors, AGB information has been derived from active sensors such as synthetic aperture radar (SAR) and light detection and ranging (LiDAR), on space-borne and airborne platforms respectively [24,25]. Indeed, LiDAR has become one of the most prominent remote sensing technologies in forest assessment [26–29]. LiDAR metrics, from both discrete return (DR) and full waveform (FW), have been shown to obtain highly accurate forest AGB and above carbon density (ACD) estimates, with no saturation issues associated with areas of high AGB [30,31]. This lack of saturation is a key benefit associated with the use of LiDAR data in tropical forest ecosystems, where traditional optical data may struggle to provide accurate estimates in areas with dense vegetation cover due to signal saturation in bands associated with high reflectance in green vegetation (such as green and near-infrared bands). Further, LiDAR structural information, in particular from LiDAR metrics related to the midcanopy forest structure, is important for assessing biomass in tropical peat swamp forest AGB estimation [9]. Despite these successes [32], LiDAR surveys over landscape scales are expensive and problematic. LiDAR systems are often limited by their spatial and temporal coverage (airborne acquisition), thus producing results best suited to sample transect datasets rather than the wall-to-wall coverage often called for in regional forestry applications, particularly when the demand is for high spatial resolutions [33,34]. To combat these limitations, many studies combine LiDAR and spaceborne optical data for landscape-scale forestry applications [35–39]. Here, LiDAR-derived forest attributes or models are commonly adopted as surrogate ground truth data. The large amount of training samples generated from LiDAR data can significantly improve the performance and accuracy in predicting forest attributes using machine learning algorithms [40,41], thus overcoming the restrictions posed by traditional field sampling methods.

This research focuses on the North Selangor Peat Swamp Forest (NSPSF), a large tropical peat swamp forest in Peninsular Malaysia under varying degrees of both growth and degradation from multiple drivers. In view of the growing international interest in tropical peatland conservation and restoration, NSPSF was under state protection with an established site-specific Integrated Management Plan (IMP) [42] set out from 2014 to 2023 to support and implement tropical peat swamp restoration. The IMP specifically targeted key areas of rehabilitation, fire prevention, and buffer zone management. To date, several IMP interventions have been implemented in NSPSF with varying degrees of success, including drain blocking, fire prevention, and forest replanting programmes. The years 2015–2018 marked a period of significant effort in the initial trial and installation of several peat swamp management and restoration activities set out by the IMP. Evidence of the impacts (both positive and negative) of these activities on the restoration of NSPSF is required to aid local stakeholders in prioritising and formulating future management strategies. In this research, we test and demonstrate the use of Sentinel-2 satellite data in delivering accurate, high-resolution AGB maps of NSPSF for the years 2015 and 2018

using a Random Forest machine learning method. Despite the proven accuracy of LiDAR data in tropical peat swamp forest AGB estimation [9] and the limitations associated with forest stand structural representation in optical data, Sentinel-2 was selected as the practical data option for this research based on data cost, coverage, and cloud contamination. A reference dataset derived from the LiDAR AGB model results by Brown et al. [9] was used as training and validation data in the Random Forest model. The resulting AGB maps will facilitate a change detection analysis to assess AGB dynamics between 2015 and 2018, providing insights into the effectiveness of peat swamp management activities in NSPSF. This evaluation is crucial for informing future management strategies and supporting international conservation goals.

2. Materials and Methods

2.1. Study Site

NSPSF is located on the flat coastal plains of northwest Selangor, Peninsular Malaysia (3°33′31N, 101°18′21E). Comprising four forest reserves—Raja Musa Forest Reserve, Sungai Karang Forest Reserve, Bukit Belata Extension Forest Reserve (partial), and Sungai Dusun Forest Reserve—NSPSF is one of the largest remaining peat swamp forests in Peninsular Malaysia [43], covering a total area of 81,304 ha. NSPSF provides a wealth of ecosystem services—such as habitat biodiversity, carbon sequestration, regulation of freshwater flow and flood mitigation, and climate regulation—that are all essential to the local livelihood of neighbouring human communities [42]. However, decades of peat swamp forest degradation and encroachment have restricted NSPSF ecosystem function and the services it can provide [44–46].

The forest is a recovering secondary mixed swamp forest in which multiple cycles of selective logging have created a complex, multi-layered canopy structure, crisscrossed by a 500 km network of log extraction canals [42,47]. The construction of the canals has scarred the forest, accelerating the drainage of the peat soil and consequently increasing fire risk for the reserve and surrounding area. The land use adjacent to the reserve is dominated by large-scale oil palm plantations. Conversion to industrial oil palm has transformed the landscape in North Selangor [48], with reserve encroachment and hydrological consequences of plantation drainage posing a serious threat to the protection and ecosystem function of NSPSF. The reserve also notably borders the Tanjung Karang Irrigation Scheme to the west, which predominantly serves the Sekinchan rice paddy fields and mining/ex-mining activities to the southeast.

As a result of destructive human activities and the degradation of tropical peat swamp forests, the Selangor State Government agreed on a 25-year moratorium on timber extraction across the State starting in 2007 [42]. Following this step toward peatland restoration and rehabilitation, the IMP was developed in 2013–2014, prepared by the Selangor State Forestry Department with technical support from the Global Environment Centre (GEC), and approved by the Selangor State Government in October 2014. This plan was a significantly updated version of a previous IMP for NSPSF incorporating research findings from within the reserve and best management practices for peat swamp conservation. The IMP specifically targeted key areas for rehabilitation, fire prevention, and buffer zone management across NSPSF, adopting a zonal approach where focused activities of restoration and conservation could be strategically directed to the areas/zones most at risk of degradation. Several IMP interventions were implemented in NSPSF with varying degrees of success, including drain blocking, the introduction of strict no-burning requirements, community-based fire prevention and patrolling programmes, and forest replanting in severely degraded sites.

2.2. Workflow

Figure 1 illustrates the workflow for estimating tropical peat swamp forest AGB across the entire NSPSF and assessing the impact of natural and anthropogenic change on the site between 2015 and 2018. This includes the extraction of Sentinel-2 model input variables

(spectral and textural), the development of a predictive model for tropical peat swamp forest AGB, and a change analysis of 2015 and 2018 AGB map outputs.

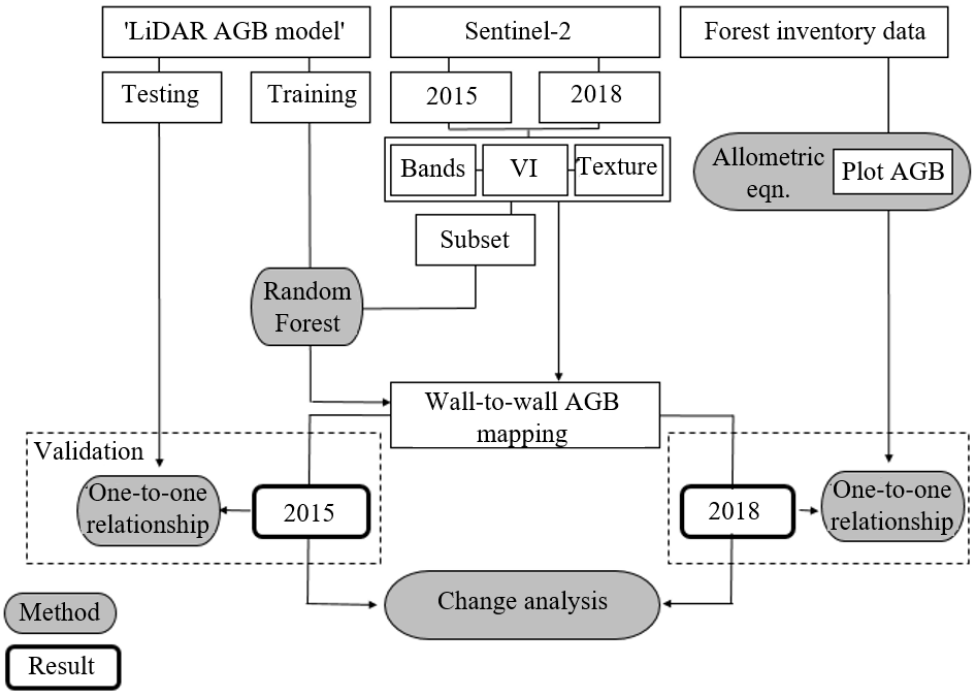


Figure 1. Workflow of the major tasks carried out in this research.

2.3. Sentinel-2 Data and Preprocessing

Sentinel-2 is an Earth observation system part of ESA's Copernicus programme—a series of satellites under the family name Sentinel with a policy of free and open-access spaceborne data. Sentinel-2 is a constellation of twin satellites, Sentinel-2A and Sentinel-2B. The pair aims to provide enhanced multispectral data with a high revisit time of 5 days [49]. The Sentinel-2 satellites carry the MSI sensor that samples across thirteen spectral bands at a spatial resolution ranging from 10 to 60 m. The MSI sensor's unique band combination importantly includes three vegetation-focused bands positioned in the Red-Edge zone (across 705–865 nm, at a 20 m spatial resolution).

Sentinel-2 MSI scenes were acquired for 31 December 2015 and 13 February 2018 (both dates fall in the region's dry season), supplied as Level 1C geocoded formatting. As Sentinel-2 Level 1C data are top-of-atmosphere reflectance, the ENVI FLAASH algorithm was applied to convert this to surface reflectance (bottom of atmosphere). MSI spectral bands with a 20 m spatial resolution (band 5, band 6, band 7, band 8a, band 11, and band 12) were resampled to 10 m by applying the nearest-neighbour interpolation algorithm. Both Sentinel-2 MSI scenes were projected to WGS 1984 UTM Zone 47N (the same projection as Brown et al. [9] NERC Airborne Research Facility LiDAR data), and key structures in the landscape (using GPS data collected in the field) were used to check the intercalibration of the two scenes.

2.4. Sentinel-2 Model Input Variables

A total of 142 spectral and textural variables were calculated to estimate the AGB of NSPSF for the two dates of interest. Spectral variables include the preprocessed Sentinel-2 MSI bands (band 2: blue (490 nm), band 3: green (560 nm), band 4: red (665 nm), band 5: vegetation Red-Edge (705 nm), band 6: vegetation Red-Edge (740 nm), band 7: vegetation Red-Edge (783 nm), band 8: near-infrared (842 nm), band 8a: narrow near-infrared (865 nm), band 11: short wave infrared (1610 nm), and band 12: short wave infrared (2190 nm)) and a selection of vegetation indices (Table 1). The selection of vegetation indices was based on their performance in past research [50,51]; these indices have proven to represent the strong

contrast in reflectance in the near infrared (NIR) by plant matter and the strong absorption by chlorophyll in the red part of the electromagnetic spectrum, essentially measuring vegetation greenness. Additionally, vegetation indices adapted to utilise the Red-Edge zone were included to take full advantage of the multiple bands covering this sensitive spectral region [52,53]. Vegetation indices were calculated in R software (version 3.5.2) using the 'Raster' package [54].

Table 1. Vegetation indices with equation and the Senitnel-2 MSI bands used.

Vegetation Index	Equation	Sentinel-2 MSI Bands Used
Normalised Difference Vegetation Index (NDVI)	= (NIR − R)/(NIR + R)	= (band 8 − band 4)/(band 8 + band 4)
Normalised Difference Vegetation Index Red-Edge band 5 (NDVI-RE5)	= (NIR − RE1)/(NIR + RE1)	= (band 8 − band 5)/(band 8 + band 5)
Normalised Difference Vegetation Index Red-Edge band 6 (NDVI-RE6)	= (NIR − RE2)/(NIR + RE2)	= (band 8 − band 6)/(band 8 + band 6)
Normalised Difference Vegetation Index Red-Edge band 7 (NDVI-RE7)	= (NIR − RE3)/(NIR + RE3)	= (band 8 − band 7)/(band 8 + band 7)
Simple Ratio (SR)	= NIR/R	= band 8/band 4
Simple Ratio Red-Edge band 5 (SR-RE5)	= NIR/RE1	= band 8/band 5
Simple Ratio Red-Edge band 6 (SR-RE6)	= NIR/RE2	= band 8/band 6
Simple Ratio Red-Edge band 7 (SR-RE7)	= NIR/RE3	= band 8/band 7
Inverted Red-Edge Chlorophyll Index (IRECI)	= (NIR − R)/(RE1/RE2)	= (band 8 − band 4)/(band 5/band 6)
Sentinel-2 Red-Edge Position (S2REP)	= 705 + 35 × ((((NIR + R)/2) − RE1)/(RE2 − RE1))	= 705 + 35 × ((((band 8 + band 4)/2) − band 5)/(band 6 − band 5))

Texture variables based on the grey-level co-occurrence matrix (GLCM) approach [55] were generated to enhance the spatial discrimination of features in the data scenes, such as tree density and linear structures in the landscape (i.e., canals). Three GLCM metrics—homogeneity, mean, and variance (Table 2)—were applied to individual Sentinel-2 MSI bands under different windows sizes (3 × 3, 5 × 5, 7 × 7, and 9 × 9 pixels) at an offset distance of 1 and averaged in all directions. Texture variables were generated in R software (version 3.5.2) using the 'glcm' package [56].

Table 2. The GLCM-based texture variables formula.

$$\text{Homogenity} = \sum_{i,j=0}^{N-1} \frac{P_{i,j}}{1+(i-j)^2}$$

$$\text{Mean} = \sum_{i,j=0}^{N-1} i\left(P_{i,j}\right)$$

$$\text{Variance} = \sum_{i,j=0}^{N-1} P_{i,j}\left(i - Mean\right)^2$$

Note: $P_{i,\,j} = {V_{i,j}}\Big/{\sum_{i,j=0}^{N-1} V_{i,j}}$, where $V_{i,j}$ is the value in the cell (i, j) (row i and column j) of the moving window and N is the number of rows or columns.

2.5. Training and Validation Data

2.5.1. 'LiDAR AGB Model'

In order to overcome the many barriers to obtaining field inventory plot data for AGB estimation, past studies have adopted LiDAR transects as surrogate plot data [35–38]. In a similar vein, this research uses the site-specific model developed by Brown et al. [9] as model training and testing data for predicting AGB for NSPSF. The predictive model and statistics presented are listed in Table 3. Based on this model, a thematic map of tropical peat swamp forest AGB was generated for a subset of LiDAR flightlines recorded by the NERC ARF team in the 2014 Malaysia campaign, gridded at 10 × 10 m spatial resolution (scale matching the Sentinel-2 MSI 10 m spatial resolution bands). It is important to note here the three-year time delay between the collection of the airborne LiDAR data (2014) and field plot inventory data (2017) used by Brown et al. [9] in developing this model. This

may introduce error into the AGB model; however, all field plots were established to be free from logging and fire, with no obvious disturbance within the three years.

Table 3. Performance of 'LiDAR AGB model' developed by Brown et al. [9]. Where AGB = above-ground biomass; H_mean = mean plot height of median energy (HOME); B50 = 50th height bincentiles; R^2 = R square; RMSE = root mean square error; rRMSE = relative root mean square error.

Predictive Model	R^2	RMSE (Mg/ha)	rRMSE (%)
AGB = 171.3732 + 14.7802 × H_mean − 1.5752 × B50	0.77	39.8	10.8

The AGB data generated from the Brown et al. [9] model, herein known as the 'LiDAR AGB model', represent an area of 9457.08 ha with high accuracy, covering just over 10% of NSPSF (Figure 2). These sections of the reserve have faced little reported large-scale forest cover change since the updated IMP implementation in 2014. The areas of the reserve covered by the 'LiDAR AGB model' support forest with a range of structural characteristics (i.e., height and density), and are thus deemed appropriate and representative as training and testing data for mapping AGB across the whole of the NSPSF (Figure 2). A simple visual check on the spatial positioning of datasets was made. Sourcing appropriate structures in the landscape as reference points was restricted due to the forest structure and data resolution (10 m), with reference points limited to clear reserve boundary lines. The spatial correspondence of datasets in this research may introduce errors into the final wall-to-wall AGB estimations.

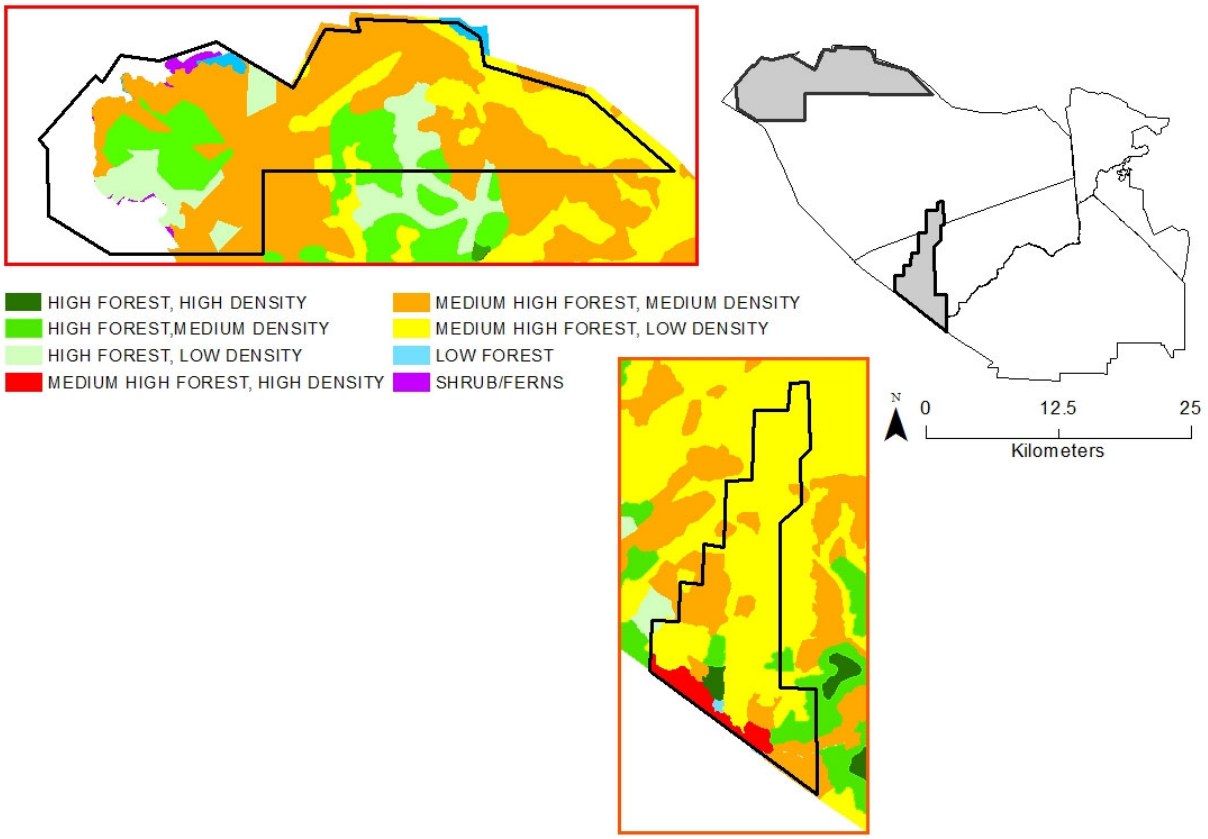


Figure 2. 'LiDAR AGB model' area coverage (black polygon border) overlaid onto forest type (forest height (high, medium, low) and forest density (high, medium, low)) results from a forest inventory undertaken in 2000 [57].

The 'LiDAR AGB model' totaled 949,119 pixels (10 m spatial resolution), of which 70% (664,383) were randomly sampled to use as training data, and the remaining 30% (284,736) were reserved for testing (Table 4).

Table 4. Summary statistics for the 'LiDAR AGB model' [9].

Sample Number	Mean	Median	SD	Minimum	Maximum
949,119	224.53	221.79	122.6242	24.02	600.00

2.5.2. Field Inventory Data

Forest inventory ground truth data were collected in 2018 to be used as validation data for the 2018 AGB model output. To estimate field AGB, 17 circular field plots with a radius of 15 m were established throughout the reserve, with a keen effort to cover areas of different locations, forest types, degradations, and management in NSPSF.

The location of the central tree, and thus the centre point of the plot, was recorded by a field GPS (Garmin GPSMAP 64), with an average horizontal error of <5 m when measurements were averaged over ten minutes. The positions of all further trees within the plot were noted relative to the centre (distance and angle). For each plot, all live trees with a diameter at breast height (DBH) of >5 cm were measured, and recognised tree species were recorded. Additionally, dependent on the top of tree visibility, selected trees of varying height classes were measured by laser height meter. Plot AGB values were calculated based on the general pan-tropical allometric equation developed by Chave et al. [58].

$$AGB = 0.0673 \times (\rho D^2 H)^{0.976}$$

where ρ = wood density (g/cm^3), D = DBH (cm) and H = height (m).

Inputs included field-measured DBH, species (to estimate wood density), and tree height when available (missing height data were retrieved from the Feldpuash et al. [59] averaged model, with the region set to Southeastern Asia). Wood density was estimated for the trees based on their taxonomy using the global wood density database (GWD) [60,61], unidentified trees or trees with a missing genus in the GWD were assigned a mean plot-level wood density value.

The 'BIOMASS' package in R software (version 3.5.2) [62] was used to run AGB estimation. AGB values were calculated for individual trees within each 15 m radius field plot and then summed to obtain total AGB plot values.

2.6. Random Forest Regression

The Sentinel-2 2015 spectral and textural variables and the training data (70% of the 'LiDAR AGB model') were used as inputs for a nonparametric data fusion machine learning algorithm, Random Forest [63]. As previously mentioned, the 'LiDAR AGB model' was developed from a LiDAR dataset captured in 2014 and forest inventory plot data collected in 2017. The temporal time difference between the 'LiDAR AGB model' and the Sentinel-2 scenes may introduce error into the Random Forest regression; however, the areas of the reserve covered were established to be free from logging and fire damage in this time period, with no obvious structural disturbance.

The Random Forest algorithm is widely used in the remote sensing community [37,38,64,65] due to its capacity to handle potentially noisy and highly correlated variables often associated with remotely sensed datasets [63,66]. Previous research [32,40] found the Random Forest method to produce superior results in comparison with other approaches, such as Support Vector Machine, k-nearest neighbour, and Gaussian processes.

Random Forest is an ensemble learning method based on classification and regression trees, this research follows the latter using the 'Ranger' package [67] within R environment software (version 3.5.2). Random Forest regression operates by constructing a large number of trees, i.e., a forest, by randomly selecting the predictor variables from the input dataset

and then calculating a mean prediction from all individual trees grown. One-third of the input data, termed the out-of-bag (OOB) sample, are left out of the bootstrap sample and are used to calculate an unbiased estimate for the retrieval error (OOB error). Within the Random Forest regression, three parameters need to be optimised: (1) ntree, the number of trees grown; (2) mtry, the number of different predictors sampled at each node; and (3) nodesize, the minimal size of the terminal nodes of the trees.

In addition to prediction, Random Forest estimates variable importance measures to rank variables by their predictive importance. The 'Ranger' package computes the permutation importance of a variable, calculated as the difference in prediction performance before and after permuting the values of the variable averaged over all trees built by the Random Forest. In each tree, OOB data are included in the variable importance calculation. Importance values are ranked and used to determine the predictor strength and influence on the Random Forest model performance. This information can then be used to tailor predictor selection by eliminating low-ranking predictor variables to produce the best predictive power and help interpret the final model.

An independent validation was performed with the test data (30% of the 'LiDAR AGB model') unseen by the model. The following statistical parameters were considered for the independent validation: R square (R^2), adjusted R square (Adj-R^2), Root Mean Square Error (RMSE), Normalised Root Mean Square Error (NRMSE) that results in a percentage (%RMSE), and Bias.

2.7. Wall-to-Wall AGB for NSPSF

Wall-to-wall peat swamp forest AGB maps over the entire reserve were generated using the Random Forest model for both the 2015 and 2018 scenes. The use of the Random Forest model, built from the subset Sentinel-2 2015 variables and 'LiDAR AGB model', to estimate AGB across the entire site for the 2018 scene was deemed appropriate as the training areas covered a good representation of the study site but importantly also covered a large area of all vegetation types. Thematic AGB maps were created at a 10 m spatial resolution (0.01 ha).

2.8. 2018 AGB Validation

The predictive ability and transferability of the Random Forest model for estimating AGB across the entire reserve for 2018 was assessed using an independent validation dataset of field inventory plot data collected in 2018. A one-to-one relationship between measured and predicted AGB values was fitted. Common statistical parameters were computed—R square (R^2), adjusted R square (Adj-R^2), Root Mean Square Error (RMSE), Normalised Root Mean Square Error (NRMSE) that results in a percentage (%RMSE), and Bias.

2.9. AGB Change Analysis

The NSPSF AGB maps generated for 2015 and 2018 (10 × 10 m pixel resolution) were used to calculate an AGB change map by subtracting the 2018 AGB map from the 2015 AGB map. The resulting AGB change map was visually analysed and interpreted with reference data acquired from the Selangor State Forestry Department and local community and conservation groups.

The following information was provided:

- Dates and locations of drain-blocking activities;
- Dates and locations of replanting programmes;
- Dates and locations of large-scale fire events;
- Locations of human hydrological interventions, e.g., clay bunds/dyke installations;
- Recent changes in land adjacent to NSPSF, e.g., road upgrades.

Interpretation of NSPSF AGB change between 2015 and 2018 was also supported by the IMP documentation and personal knowledge of the reserve obtained from frequent field campaigns in NSPSF.

3. Results

3.1. Random Forest Model Performance

The variable importance rankings, based on the permutation variable importance approach, were used to improve the predictive performance of the Random Forest model through a progressive backward feature elimination (i.e., removing the lowest ranked variable until the model was optimised). The full set of predictor variables generated from the 2015 subset Sentinel-2 data (n = 142) was reduced (n = 62) to yield the highest predictive performance in the final Random Forest model for estimating tropical peat swamp forest AGB in NSPSF. The variables that ranked highest in the final optimised Random Forest model (Figure 3) were predominantly based on the variance and mean texture variables, at a variety of window sizes, applied to Sentinel-2 MSI bands positioned in key features of green vegetation spectral response (b3 = Green, b4 = Red, b5 = Red-Edge, b6 = Red-Edge, and b8a = Narrow-NIR). Additionally, vegetation indices incorporating the Sentinel-2 Red-Edge bands also ranked highly in model importance, for example, NDVI-RE5, NDVI-RE6, SR-RE5, and SR-RE6.

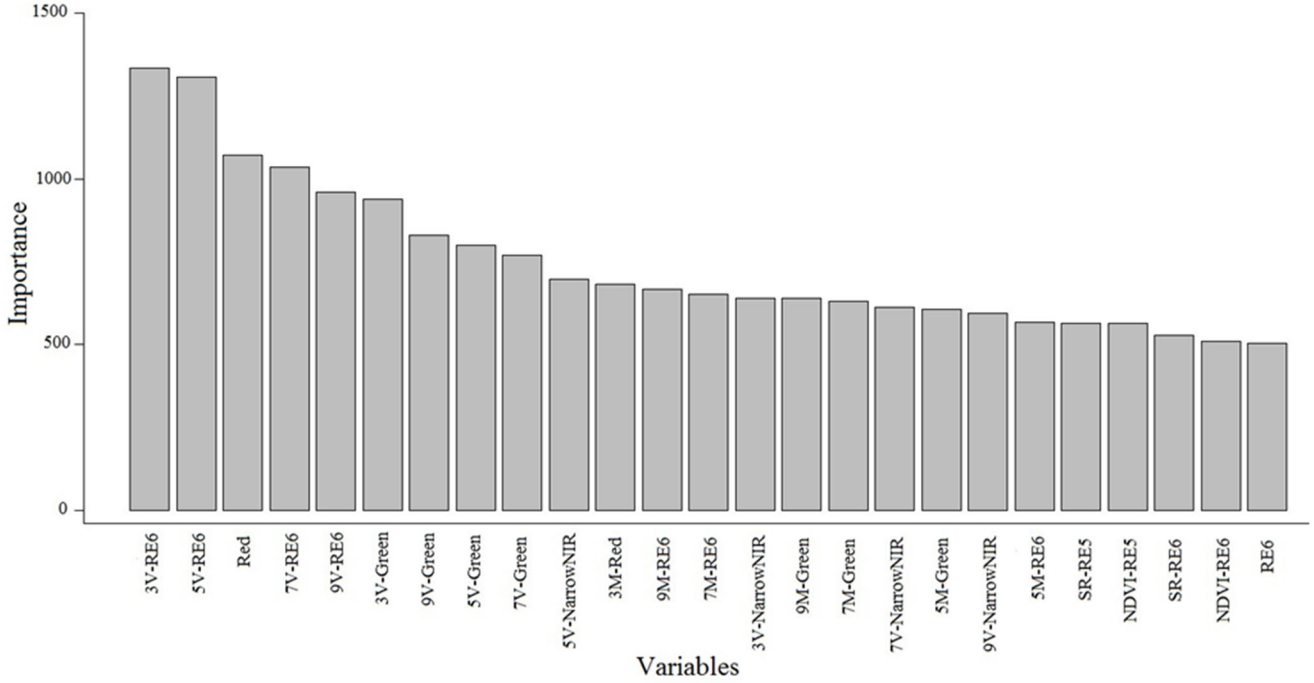


Figure 3. The top 25 ranked variables from the optimised Random Forest model based on the permutation variable importance (Importance). Where 3V-RE6 = 3 × 3 Variance Red-Edge band 6; 5V-RE6 = 5 × 5 Variance Red-Edge band 6; Red = band 4; 7V-RE6 = 7 × 7 Variance Red-Edge band 6; 9V-RE6 = 9 × 9 Variance Red-edge 6; 3V-Green = 3 × 3 Variance Green band 3; 9V-Green = 9 × 9 Variance Green band 3; 5V-Green = 5 × 5 Variance Green band 3; 7V-Green = 7 × 7 Variance Green band 3; 5V-NarrowNIR = 5 × 5 Variance Narrow NIR band 8a; 3M-Red = 3 × 3 Mean Red band 4; 9M-RE6 = 9 × 9 Mean Red-Edge band 6; 7M-RE6 = 7 × 7 Mean Red-Edge band 6; 3V-NarrowNIR = 3 × 3 Variance Narrow NIR band 8a; 9M-Green = 9 × 9 Mean Green band 3; 7M-Green = 7 × 7 Mean Green band 3; 7V-NarrowNIR = 7 × 7 Variance Narrow NIR band 8a; 5M-Green = 5 × 5 Mean Green band 3; 9V-NarrowNIR = 9 × 9 Variance Narrow NIR band 8a; 5M-RE6 = 5 × 5 Mean Red-Edge band 6; SR-RE5 = Simple Ratio Index band 5; NDVI-RE5 = Normalised Difference Vegetation Index Red-Edge band 5; SR-RE6 = Simple Ratio Index band 6; NDVI-RE6 = Normalised Difference Vegetation Index Red-Edge band 6; RE6 = Red-Edge band 6.

The Random Forest algorithm parameters, ntrees and mtyr, were also adjusted to optimise the model. The Random Forest model was set to ntrees—1800 and mtry—21.

3.2. Predictive Performance of the Random Forest Model

The Random Forest model with optimised input variables (n = 62) and parameter adjustments produced a good plausible result (R^2 = 0.80; RMSE = 55.2 Mg/ha) (Table 5). The relationship between observed AGB ('LiDAR AGB model' testing data) and predicted AGB is presented in Figure 4. Figure 4 clearly displays issues around the lowest observed AGB values overestimating AGB and the highest observed AGB values underestimating AGB; however, these represent a low proportion of the 284,736 validation points. These issues could be an effect of the limited sensitivity of satellite sensors to variations in canopy height and structure.

Table 5. Performance of optimised Random Forest model on an independent validation dataset. Where R^2 = R square; Adj-R^2 = adjusted R square; RMSE = root mean square error; %RMSE = percentage normalised root mean square error.

Number of Validation Points	R^2	Adj-R^2	RMSE (Mg/ha)	%RMSE	Bias
284,736	0.80	0.80	55.2	24.6%	−0.15

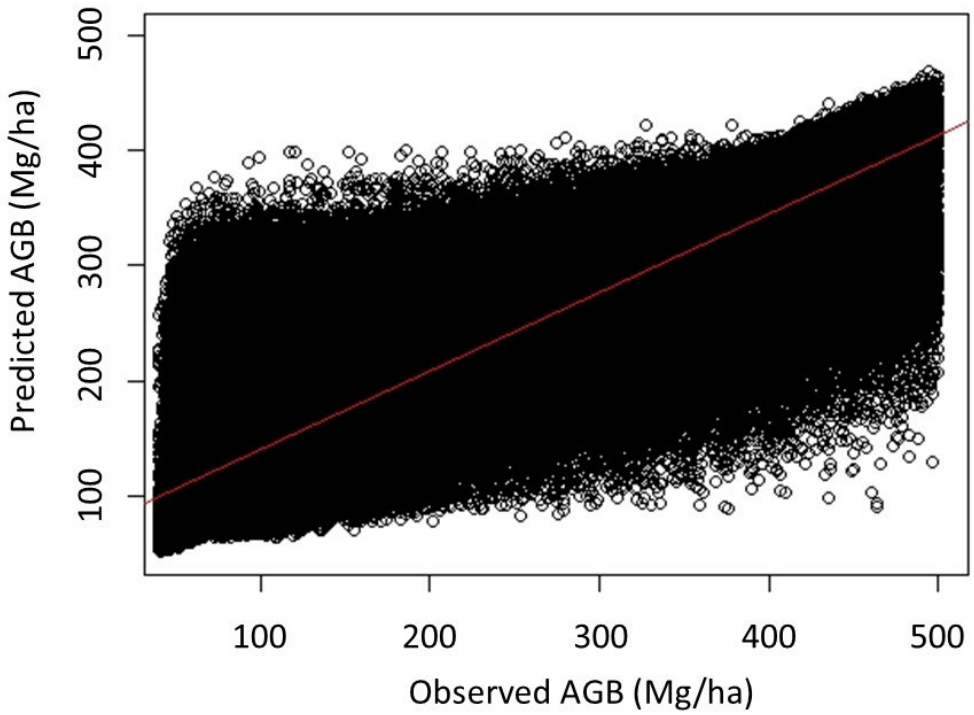


Figure 4. Observed vs. predicted aboveground biomass (AGB) using the optimised Random Forest model with an independent validation dataset.

3.3. Wall-to-Wall AGB Maps

The wall-to-wall AGB map produced for the year 2015 using the optimised Random Forest model can be seen in Figure 5. Figure 5 displays the distinct AGB spatial distribution within the NSPSF reserve in 2015, depicting areas of different tropical peat swamp forest types and densities, as well as highlighting areas of potential disturbance or degradation. The mean predicted tropical peat swamp forest AGB estimate was 246 Mg/ha, with a range of 25–599 Mg/ha.

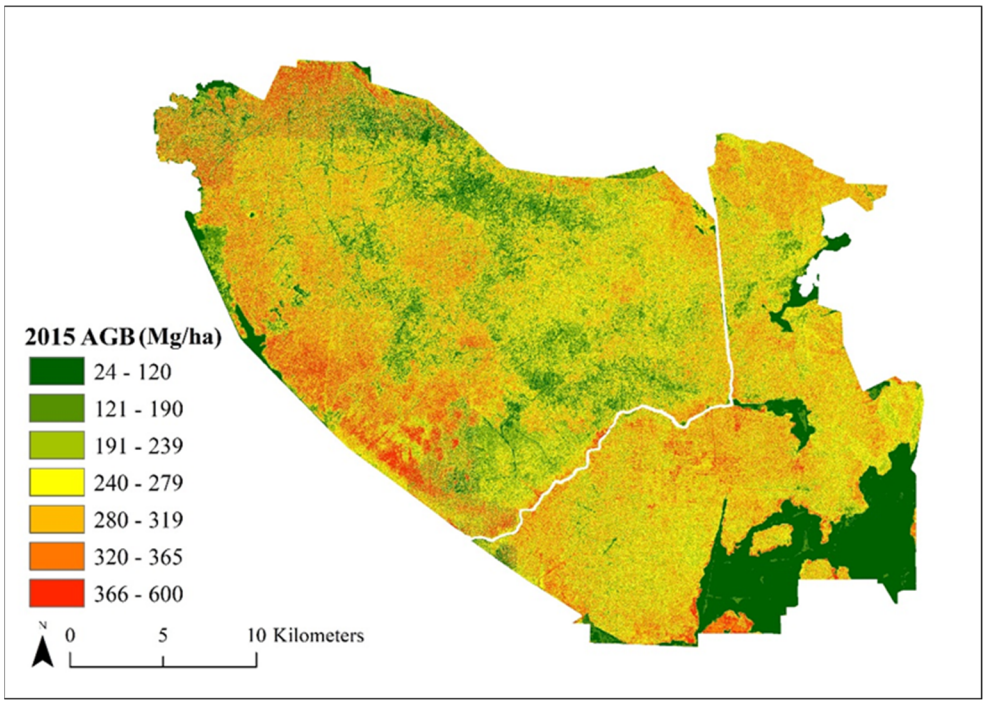


Figure 5. The 2015 aboveground biomass (AGB) (Mg/ha) estimated for NSPSF reserve calculated from the optimised Random Forest model, at a 10 m (0.01 ha) spatial resolution.

The wall-to-wall AGB map produced for the year 2018 applying the optimised Random Forest model built from the 2015 subset Sentinel-2 variables and 'LiDAR AGB model' data can be seen in Figure 6. This presents the AGB spatial distribution across the NSPSF reserve for 2018, where visual analysis of the map highlights the variety of tropical peat swamp forest vegetation cover. The mean predicted tropical peat swamp forest AGB estimate was 253 Mg/ha, with a range of 25–584 Mg/ha.

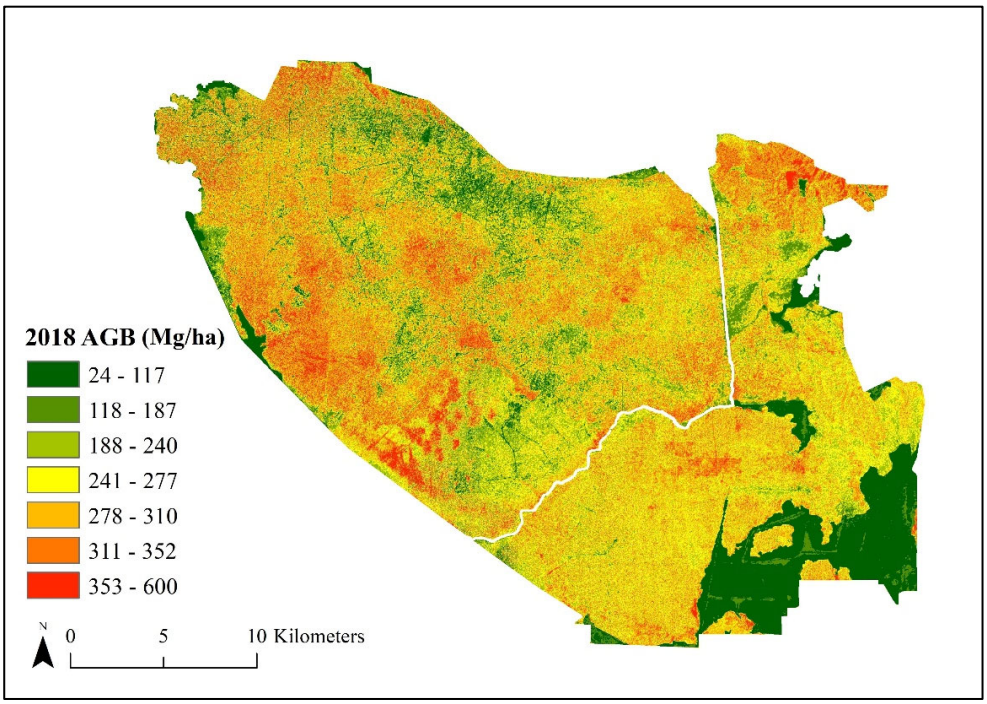


Figure 6. The 2018 aboveground biomass (AGB) (Mg/ha) estimates for NSPSF reserve calculated from the optimised Random Forest model, at a 10 m (0.01 ha) spatial resolution.

3.4. 2018 AGB Independent Validation

The validation results from the one-to-one relationship between predicted AGB and observed AGB (field plots) presented a strong agreement (R^2 = 0.92; RMSE = 23.4 Mg/ha) (Table 6). The relationship between observed AGB (field data) and predicted AGB for 2018 is presented in Figure 7. Overall, the optimised Random Forest model accurately mapped AGB across NSPSF using Sentinel-2 spectral and textural variables for 2018. This result seems counterintuitive to the findings of Brown et al. [9] ('LiDAR AGB model' reported R^2 = 0.77 (Table 3)) and past research reporting LiDAR as the most accurate data source for AGB estimation [32]. However, this reported high R^2 may be a result of the small sample size for the test set (17 field plots), which can lead to unstable results. A larger dataset covering a wider and more varied range of AGB values, in particular for lower AGB (<150 Mg/ha) and high AGB (>400 Mg/ha), may expose a less accurate AGB estimation for 2018.

Table 6. Independent validation results from 2018 AGB estimation. Where: R^2 = R square; Adj-R^2 = adjusted R square; RMSE = root mean square error; %RMSE = percentage normalised root mean square error.

Number of Validation Points	R^2	Adj-R^2	RMSE (Mg/ha)	%RMSE	Bias
17	0.92	0.92	23.4	8.73%	−5.45

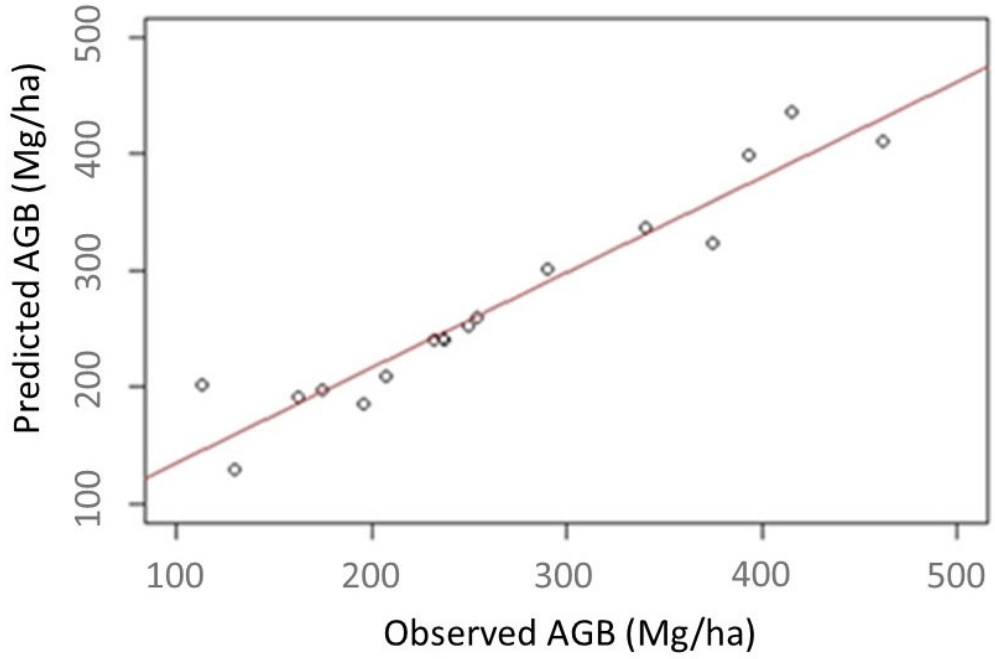


Figure 7. Observed vs. predicted aboveground biomass (AGB) using the 2018 predicted AGB results and field inventory estimated AGB

3.5. Change Analysis

The change in AGB distribution and abundance is presented in Figure 8. The interpretation and analyses of the AGB change map using reference datasets and expert knowledge of the site revealed a number of key areas of change in NSPSF. Table 7 identifies the key areas of change, in both AGB gain and loss, alongside a review of the land management activities and disturbances that have impacted these areas.

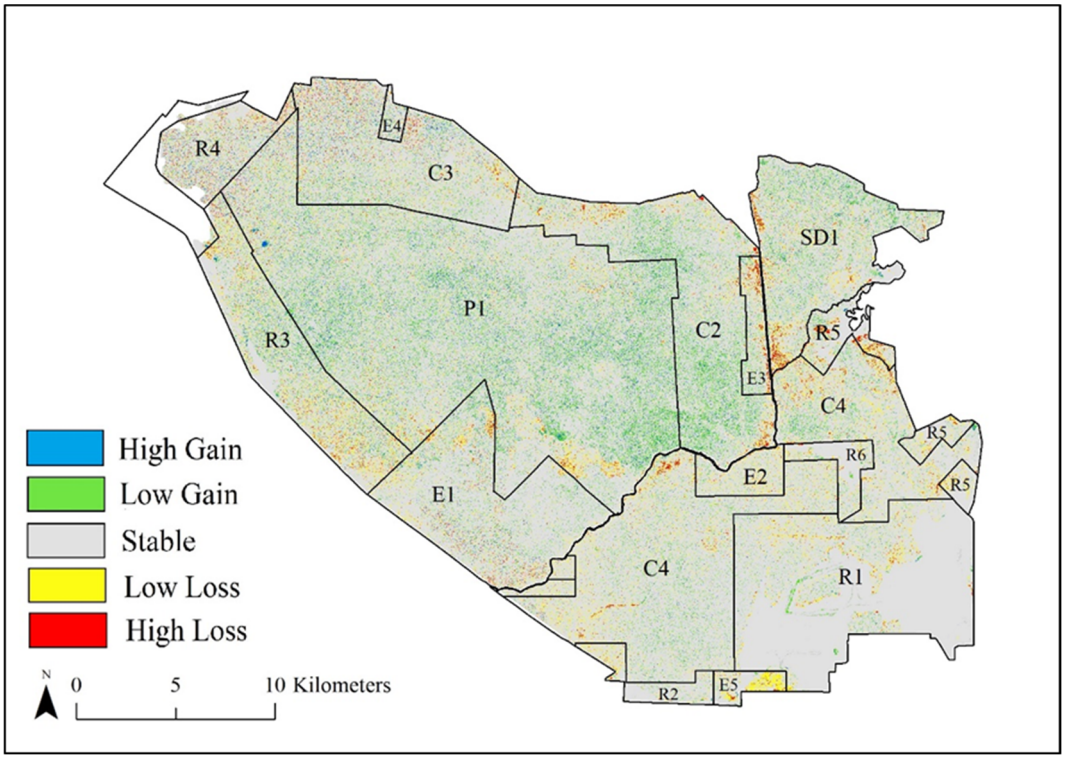


Figure 8. Aboveground biomass (AGB) change between the years 2015 and 2018 for the reserve. Classified as high gain, low gain, stable, low loss, and high loss. The black polygon border shows the prominent management zones outlined in the Integrated Management Plan documentation. Management zones: Agroforestry (A), Community Forest (CF), Biodiversity Conservation (C), Ecotourism, Recreation and Education (E), Water Catchment (P), Rehabilitation (R), Sungai Dusun Wildlife Reserve (SD).

Table 7. Prominent management zones of change in NSPSF and the associated IMP interventions and proposed regeneration strategies.

AGB Gain	P1	This large central section of NSPSF has been designated by the IMP as a water catchment forest. P1 covers the deepest areas of peat soil and potential peat domes; this area plays a vital role in water storage and the regulation function of NSPSF. Between the years 2015 and 2018, the key goals of the management designation were forest protection and blocking of the main drainage canals to encourage natural regeneration. The AGB gains provide evidence of the successful regeneration of P1 and present a good example of sustainable management of tropical peat swamp forest.
	C2	This section of NSPSF covers both central areas of the forest (neighbouring P1) and areas of forest on the reserve boundary. These areas have been designated by the IMP as a conservation zone. In the past, this area was heavily degraded by intensive logging activities and associated drainage; however, in 2018, the forest was recovering well, supported by AGB gain values (Figure 8). Although the majority of C2 shows AGB gain, there is a focused area of AGB loss at the northern boundary (Figure 9). This is thought to be in association with peat drainage and potential peat subsidence linked to ex-logging canals that connect to drains along the Tanjong Malim–Sg Besar road (road upgrade, high drains, and culverts) and oil palm plantations.
AGB Loss	E5	This section of NSPSF covers a relatively small area, designated in the IMP as an education and ecotourism zone. However, it is adjacent to zones R2 and R1, which are areas of severely degraded peat swamp annually affected by large scale fire events. E5 and the neighbouring R2 and R1 zones underwent major management interventions between 2015 and 2018, including large-scale drain blocking campaigns and replanting schemes (Figure 10); however, frequent fire events have hampered recovery efforts, seen by the AGB loss in E5. The loss of AGB in E5 may also be linked to overdrainage in adjacent oil palm outside of the forest reserve boundary affecting water levels in the forest reserve.
	R3	This section covers the western boundary of the reserve directly adjacent to the main irrigation canal of the IADA Rice Scheme. It is designated in the IMP as a rehabilitation zone. The area was negatively impacted by the construction of a peat/clay bund in 2010, which prevented water flow from the forest to the main irrigation canal. The artificially high water flow levels led to significant tree death and impacted the integrity of the peat soil structure. In 2011, culverts were installed in an effort to restore the natural hydrology of the area; however, these were again too high and flooded the forest leading to further water management adjustments in 2012. Although efforts of regeneration and water table recovery have been made in this section, it is evident that these areas bordering the reserve still face significant forest loss.

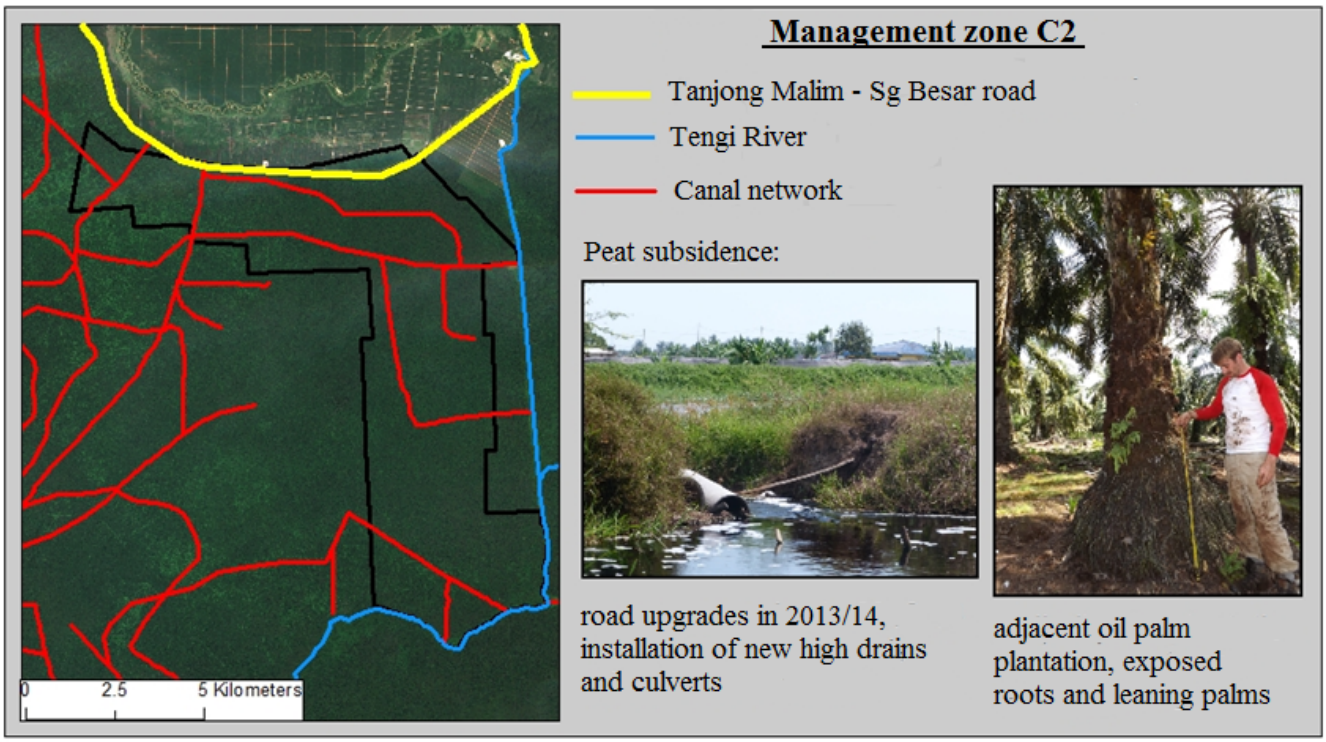


Figure 9. Management zone C2 illustrated with cause and evidence of peat swamp degradation.

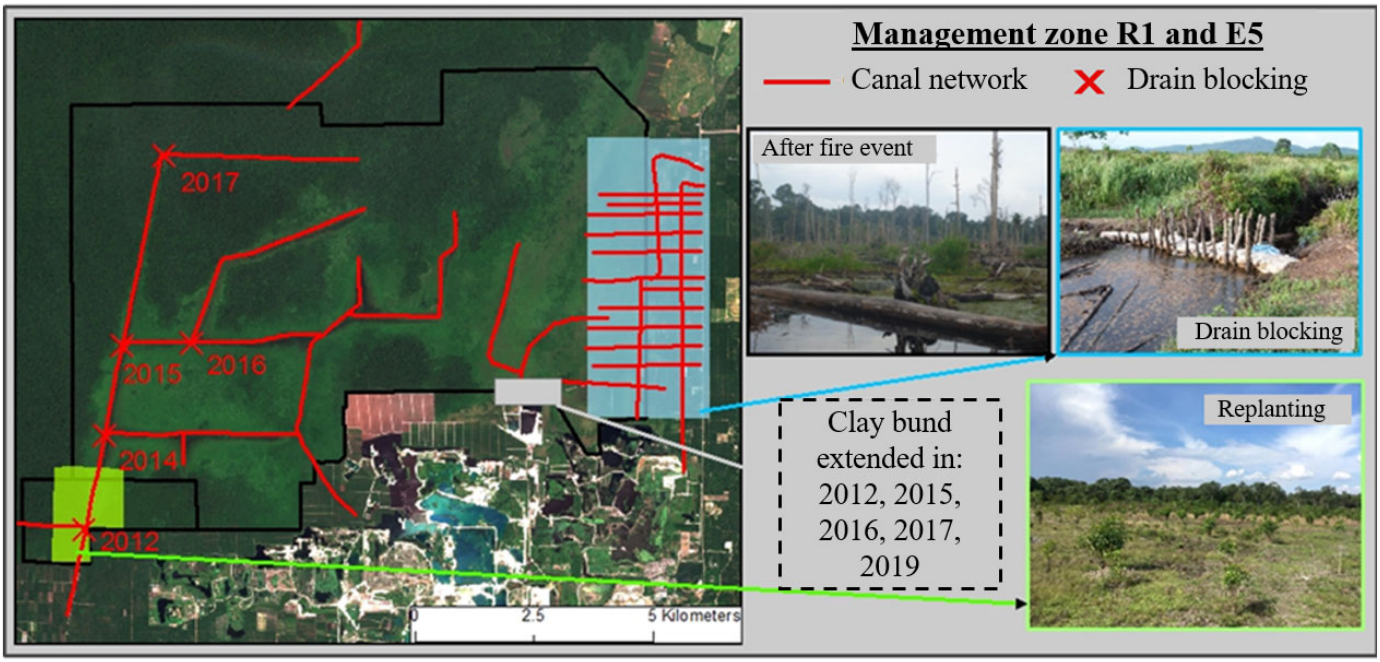


Figure 10. Management zone R1 and E5 illustrated with past restoration interventions.

4. Discussion

Planning and management to restore and conserve tropical peat ecosystems require spatially explicit and timely estimates of AGB, in particular for tracking the impacts of any restoration interventions [6]. As one of the largest remaining tropical peat swamp forests in Peninsular Malaysia, NSPSF has been recognised for its global significance as a carbon store [68–70]. As a result, its ecosystem health and security are of immense importance. The predictive Random Forest model and AGB maps presented in this research provide a quantitative tool for peat swamp forest management in NSPSF reserve, with the poten-

tial to help support current and future multi-stakeholder community-based restoration activities [71]. Additionally, it affords the ability to isolate key areas of degradation (both anthropogenic and natural), which can aid in prioritising and formulating sustainable management strategies.

The time period under investigation in this research (2015–2018) marks a focused period of restoration and regeneration efforts in the NSPSF reserve. The results from the AGB change analysis demonstrate an overall increase in tropical peat swamp AGB during these years, where the total amount of estimated AGB stored in NSPSF increased from 19.3 Tg in 2015 to an estimated 19.8 Tg in 2018, totals comparable to other AGB estimates conducted in tropical forests of similar size and density in Southeast Asia [8]. Despite this positive result, areas of concern remain within the reserve where continued AGB losses occurred, in particular toward the southeast corner of the reserve. The major factors implicating tropical peat swamp forest recovery and regeneration for NSPSF are drainage (both within the reserve and as a result of land use adjacent to the reserve) and large-scale fire events. Drainage from the estimated 500 km network of canals within the reserve, as well as a result of adjacent oil palm plantation development and ex-mining activities, continues to stress this vulnerable ecosystem [44]. Altering the natural balance of the water table, in combination with frequent large-scale fire events [72], can drive a negative feedback loop in tropical peatland ecosystems, affecting their function and resilience to further degradation [1,73]. The current canal-blocking activities and water table management efforts [74,75] must be monitored and extended throughout the entire reserve. Only by rewetting the peat can hydrological functions be restored, peat oxidation decreased, and fire risk reduced in NSPSF. In light of our results, it is encouraging to learn that the Selangor State Government, with technical assistance from the Global Environment Center, is currently updating and extending the IMP to 2033. The IMP revision will draw on the results from this research (Faizal Parish, pers comm May 2024). It is important to note that recovery can be a slow process, particularly when analysing AGB trends and dynamics at this scale, as large-scale fire events will have a short but dramatic impact, which can form a dominant marker in time series analysis when compared with long-term forest regeneration. It is therefore important to have more long-term (+5 years) studies on tropical peat swamp restoration which correspond with typically longer-term IMPs (i.e., 10 years) to analyse which methods are the most successful in tropical peat recovery [73,76]. This is an area of future work in which remote sensing technology could be usefully integrated.

The Random-Forest-based method used in this research shows great potential to upscale AGB estimates, derived from the 'LiDAR AGB model', to larger landscape-scale areas with Sentinel-2 spectral and textural variables. The variable importance rankings were used to assess the influence of Sentinel-2 spectral and textural inputs on the predictive performance of the Random Forest model. This research found a tailored variable selection approach improved predictions of AGB, this is in line with previous research applying the Random Forest algorithm to remotely sensed data [77,78]. The inclusion of textural variables had the greatest importance for modelling AGB in tropical peat swamp forests using optical satellite data (Figure 3). Texture values in an image allow the spatial heterogeneity to be evaluated, this can provide information on the distinct structure and development stages of forest stands. In particular, textural variables applied to Sentinel-2 bands positioned in known green vegetation spectral features, for example, the Red-Edge (bands 5, 6, and 7) and narrow near-infrared bands (band 8a), improved AGB estimation. The advantage of Sentinel-2 bands covering the Red-Edge zone has been noted in a number of forestry studies [22,52,79]. Additionally, vegetation indices incorporating Red-Edge bands proved to be important for modelling AGB. Laurin et al. [80] suggested that the use of vegetation indices incorporating the Red-Edge bands may help mitigate the saturation issues associated with the use of traditional vegetation indices in the tropics. A potential opportunity to improve AGB modelling in future work could be the inclusion of textural variables applied to vegetation indices incorporating Red-Edge bands, combining the bene-

fits of both approaches. Past research has successfully explored the use of combining both spectral and spatial techniques, namely texture measurement and image ratio [81].

It is well documented that the spatial distribution and sample size of training data have considerable influence on the accuracy of model predictions [32,82,83]. Here, the research adopted the results from a model developed by Brown et al. [9] as training and validation data in replacement of traditional field inventory plots. Errors introduced in the model development by Brown et al. [9] will inevitably influence the overall performance of the Random Forest model and AGB map outputs produced in this research. Although it must be stressed that the 'LiDAR AGB model' sample size and heterogeneity are considerably larger and better distributed than could be attained from a field-based programme covering the same spatial and temporal scope, it is also important to note that both the 'LiDAR AGB model' dataset and the forest inventory plot estimated AGB values are reference datasets and do not represent actual measurement of AGB; only destructive sampling techniques can afford this. As previously discussed, potential errors may also have been introduced into the AGB models through temporal discrepancies between the 'AGB LiDAR model' and the Sentinel-2 2015 scene, and additionally by geo-correlation issues between datasets. Combined, significant deviations from 'true' AGB values may occur.

Remote sensing has played a vital role in practical conservation management [84–86], establishing baselines for the extent and characteristics of ecosystems and their services, as well as quantifying degradation and subsequent recovery associated with both natural and anthropogenic events or processes. There are a number of trade-offs associated with the use of different remote sensing technologies and sources (such as data acquisition cost, coverage, and platform considerations), along with their associated level of data complexity and processing expertise. Although alternative remote sensing technology such as LiDAR has been proven to be superior in AGB estimation in previous research [32], optical spaceborne data remains a practical option for conservation management research applications [51,87].

Spaceborne optical data such as the Landsat series have long served as a major data source for ecosystem assessment and management [88,89]. The remote sensing community is in a golden age of spaceborne sensor technology, in particular for ecosystem structural mapping and biomass prediction [90], with the next generation of spaceborne optical sensors (e.g., ESA's Sentinel-2 and NASA/USGS's Landsat-9), LiDAR profilers (NASA's ICESat-2, NASA's GEDI, and JAXA's MOLI) and SAR sensors (e.g., ESA's BIOMASS, NASA/ISRO's NISAR, and ESA's Sentinel-1) set to provide a diverse range of datasets specifically designed for AGB assessment at a level of detail and temporal frequency never recorded before. Additionally, opportunities in high/very high spatial resolution satellite data have emerged from constellations of microsats [91,92]. These novel sensors operate at a low orbit and a comparatively low cost and thus can be deployed in large numbers. The performance of microsats is rapidly evolving [93,94], for example, Planet Labs has deployed a constellation of 100+ Doves microsats [95]. With a daily 3–5 m data resolution, the Planet Labs constellation has been flagged as an important data resource for assessing AGB, carbon stocks, and emissions at a high spatial and temporal frequency [96]. The field of remote sensing continues to evolve and revolutionise the way we view Earth's surface, leading to countless advances at the ground level in both scientific knowledge and practical application. To this end, supporting data are required to tackle global issues such as sustainable land recovery and conservation (SDG 15).

5. Conclusions

We conclude that the Random Forest algorithm is a useful and robust method for estimating AGB with Sentinel-2-derived spectral and textural predictor variables and a large, heterogeneous training dataset. The approach set out in this research provided a good opportunity to assess the success and unexpected consequences of different restoration activities (for example, drainage and replanting programmes) on AGB dynamics in NSPSF (2015–2018). Quantitatively, we observed an increase in the total estimated AGB stored

in NSPSF from 19.3 Tg in 2015 to approximately 19.8 Tg in 2018. This positive trend highlights the potential success of ongoing conservation efforts but also underscores areas of concern, particularly in the southeast corner of the reserve where AGB losses persisted. These findings underscore the critical need for up-to-date, spatially explicit ecological data to inform the sustainable management and restoration of degraded tropical peatlands. Continued monitoring of AGB across NSPSF could create an archive of landscape-scale datasets representative of this ongoing period of land management change, allowing a better understanding of the complex processes of a recovering peatland ecosystem and aiding in the development of best practice peatland restoration.

Author Contributions: Conceptualisation, C.B.; methodology, C.B.; validation, C.B. and M.J.L.; formal analysis, C.B.; investigation, C.B.; writing—original draft preparation, C.B.; writing—review and editing, C.B., D.B., S.S. and F.P.; supervision, D.B. and S.S. All authors have read and agreed to the published version of the manuscript.

Funding: This work was supported by the Natural Environment Research Council [NE/L002604/1], under the Envision DTP. Additional support from the University of Nottingham. The funders had no role in study design, data collection and analysis, decision to publish, or preparation of the manuscript.

Data Availability Statement: The raw data supporting the conclusions of this article will be made available by the authors on request.

Acknowledgments: We are very grateful to the Selangor State Forestry Department for granting reserve access, providing field ranger support for data collection, and sharing their expert knowledge and experiences working in the reserve.

Conflicts of Interest: The authors declare no conflicts of interest.

References

1. Evers, S.; Yule, C.M.; Padfield, R.; O'Reilly, P.; Varkkey, H. Keep wetlands wet: The myth of sustainable development of tropical peatlands–implications for policies and management. *Glob. Chang. Biol.* **2017**, *23*, 534–549. [CrossRef] [PubMed]
2. Page, S.E.; Hooijer, A. In the line of fire: The peatlands of Southeast Asia. *Philos. Trans. R. Soc. B Biol. Sci.* **2016**, *371*, 20150176. [CrossRef]
3. Miettinen, J.; Shi, C.; Liew, S.C. Two decades of destruction in Southeast Asia's peat swamp forests. *Front. Ecol. Environ.* **2012**, *10*, 124–128. [CrossRef]
4. Murdiyarso, D.; Lilleskov, E.; Kolka, R. Tropical peatlands under siege: The need for evidence-based policies and strategies. *Mitig. Adapt. Strateg. Glob. Chang.* **2019**, *24*, 493–505. [CrossRef]
5. Wijedasa, L.S.; Jauhiainen, J.; Könönen, M.; Lampela, M.; Vasander, H.; Leblanc, M.C.; Evers, S.; Smith, T.E.L.; Yule, C.M.; Varkkey, H.; et al. Denial of long-term issues with agriculture on tropical peatlands will have devastating consequences. *Glob. Chang. Biol.* **2017**, *23*, 977–982. [CrossRef]
6. Padfield, R.; Waldron, S.; Drew, S.; Papargyropoulou, E.; Kumaran, S.; Page, S.; Gilvear, D.; Armstrong, A.; Evers, S.; Williams, P.; et al. Research agendas for the sustainable management of tropical peatland in Malaysia. *Environ. Conserv.* **2015**, *42*, 73–83. [CrossRef]
7. Hiraishi, T.; Krug, T.; Tanabe, K.; Srivastava, N.; Baasansuren, J.; Fukuda, M.; Troxler, T.G. *2013 Supplement to the 2006 IPCC Guidelines for National Greenhouse Gas Inventories: Wetlands*; IPCC: Geneva, Switzerland, 2014.
8. Asner, G.P.; Brodrick, P.G.; Philipson, C.; Vaughn, N.R.; Martin, R.E.; Knapp, D.E.; Heckler, J.; Evans, L.J.; Jucker, T.; Goossens, B.; et al. Mapped aboveground carbon stocks to advance forest conservation and recovery in Malaysian Borneo. *Biol. Conserv.* **2018**, *217*, 289–310. [CrossRef]
9. Brown, C.; Boyd, D.S.; Sjögersten, S.; Clewley, D.; Evers, S.L.; Aplin, P. Tropical peatland vegetation structure and biomass: Optimal exploitation of airborne laser scanning. *Remote Sens.* **2018**, *10*, 671. [CrossRef]
10. Saragi-Sasmito, M.F.; Murdiyarso, D.; June, T.; Sasmito, S.D. Carbon stocks, emissions, and aboveground productivity in restored secondary tropical peat swamp forests. *Mitig. Adapt. Strateg. Glob. Chang.* **2019**, *24*, 521–533. [CrossRef]
11. Vijayanathan, J.; Ishak, M.; Parlan, I.; Omar, H.; Haruna, A.O.; Lion, M.; Hassan, M.; Jong, R.; Samah, A. Temporal patterns control carbon balance in forest and agricultural tropical peatlands in North Selangor, Malaysia. *iForest-Biogeosciences For.* **2021**, *14*, 362. [CrossRef]
12. Pan, Y.; Birdsey, R.A.; Fang, J.; Houghton, R.; Kauppi, P.E.; Kurz, W.A.; Phillips, O.L.; Shvidenko, A.; Lewis, S.L.; Canadell, J.G.; et al. A large and persistent carbon sink in the world's forests. *Science* **2011**, *333*, 988–993. [CrossRef] [PubMed]
13. Lu, D. The potential and challenge of remote sensing-based biomass estimation. *Int. J. Remote Sens.* **2006**, *27*, 1297–1328. [CrossRef]

14. Asner, G.P.; Mascaro, J.; Muller-Landau, H.C.; Vieilledent, G.; Vaudry, R.; Rasamoelina, M.; Hall, J.S.; van Breugel, M. A universal airborne LiDAR approach for tropical forest carbon mapping. *Oecologia* **2012**, *168*, 1147–1160. [CrossRef]
15. European Space Agency. *BIOMASS Report for Mission Selection May 2012*; Report No.: SP-1324/1; European Space Agency: Paris, France, 2012.
16. Corona, P. Consolidating new paradigms in large-scale monitoring and assessment of forest ecosystems. *Environ. Res.* **2016**, *144*, 8–14. [CrossRef]
17. Verkerk, P.J.; Mavsar, R.; Giergiczny, M.; Lindner, M.; Edwards, D.; Schelhaas, M.J. Assessing impacts of intensified biomass production and biodiversity protection on ecosystem services provided by European forests. *Ecosyst. Serv.* **2014**, *9*, 155–165. [CrossRef]
18. Gibbs, H.K.; Brown, S.; Niles, J.O.; Foley, J.A. Monitoring and estimating tropical forest carbon stocks: Making REDD a reality. *Environ. Res. Lett.* **2007**, *2*, 045023. [CrossRef]
19. Huang, S.; Ramirez, C.; McElhaney, M.; Evans, K. F3: Simulating spatiotemporal forest change from field inventory, remote sensing, growth modeling, and management actions. *For. Ecol. Manag.* **2018**, *415*, 26–37. [CrossRef]
20. White, J.C.; Coops, N.C.; Wulder, M.A.; Vastaranta, M.; Hilker, T.; Tompalski, P. Remote sensing technologies for enhancing forest inventories: A review. *Can. J. Remote Sens.* **2016**, *42*, 619–641. [CrossRef]
21. Pandit, S.; Tsuyuki, S.; Dube, T. Estimating above-ground biomass in sub-tropical buffer zone community forests, Nepal, using Sentinel 2 data. *Remote Sens.* **2018**, *10*, 601. [CrossRef]
22. Majasalmi, T.; Rautiainen, M. The potential of Sentinel-2 data for estimating biophysical variables in a boreal forest: A simulation study. *Remote Sens. Lett.* **2016**, *7*, 427–436. [CrossRef]
23. Lu, M.; Hamunyela, E.; Verbesselt, J.; Pebesma, E. Dimension reduction of multi-spectral satellite image time series to improve deforestation monitoring. *Remote Sens.* **2017**, *9*, 1025. [CrossRef]
24. Waqar, M.M.; Sukmawati, R.; Ji, Y.; Sri Sumantyo, J.T. Tropical PeatLand forest biomass estimation using polarimetric parameters extracted from RadarSAT-2 images. *Land* **2020**, *9*, 193. [CrossRef]
25. Berninger, A.; Siegert, F. The potential of ICESat-2 to identify carbon-rich peatlands in Indonesia. *Remote Sens.* **2020**, *12*, 4175. [CrossRef]
26. Urbazaev, M.; Thiel, C.; Cremer, F.; Schmullius, C. Assessment of the mapping of aboveground biomass and its uncertainties using field measurements, airborne lidar and satellite data in Mexico. In Proceedings of the IGARSS 2018-2018 IEEE International Geoscience and Remote Sensing Symposium, Valencia, Spain, 22–27 July 2018; pp. 8793–8796.
27. Coomes, D.A.; Dalponte, M.; Jucker, T.; Asner, G.P.; Banin, L.F.; Burslem, D.F.; Lewis, S.L.; Nilus, R.; Phillips, O.L.; Phua, M.-H.; et al. Area-based vs tree-centric approaches to mapping forest carbon in Southeast Asian forests from airborne laser scanning data. *Remote Sens. Environ.* **2017**, *194*, 77–88. [CrossRef]
28. Ni-Meister, W.; Lee, S. Allometric Relationship between Full Waveform LiDAR measurements and Above-ground Biomass. In *AGU Fall Meeting Abstracts*; ADS: Cambridge, MA, USA, 2016; Volume 2016, p. B44C-07.
29. Thapa, R.B.; Watanabe, M.; Motohka, T.; Shiraishi, T.; Shimada, M. Calibration of aboveground forest carbon stock models for major tropical forests in central Sumatra using airborne LiDAR and field measurement data. *IEEE J. Sel. Top. Appl. Earth Obs. Remote Sens.* **2014**, *8*, 661–673. [CrossRef]
30. Zhao, K.; Popescu, S.; Nelson, R. Lidar remote sensing of forest biomass: A scale-invariant estimation approach using airborne lasers. *Remote Sens. Environ.* **2009**, *113*, 182–196. [CrossRef]
31. Næsset, E.; Gobakken, T. Estimation of above-and below-ground biomass across regions of the boreal forest zone using airborne laser. *Remote Sens. Environ.* **2008**, *112*, 3079–3090. [CrossRef]
32. Fassnacht, F.E.; Hartig, F.; Latifi, H.; Berger, C.; Hernández, J.; Corvalán, P.; Koch, B. Importance of sample size, data type and prediction method for remote sensing-based estimations of aboveground forest biomass. *Remote Sens. Environ.* **2014**, *154*, 102–114. [CrossRef]
33. Mitchard, E.T.; Saatchi, S.S.; White, L.J.; Abernethy, K.A.; Jeffery, K.J.; Lewis, S.L.; Collins, M.; Lefsky, M.A.; Leal, M.E.; Woodhouse, I.H.; et al. Mapping tropical forest biomass with radar and spaceborne LiDAR in Lopé National Park, Gabon: Overcoming problems of high biomass and persistent cloud. *Biogeosciences* **2012**, *9*, 179–191. [CrossRef]
34. Boudreau, J.; Nelson, R.F.; Margolis, H.A.; Beaudoin, A.; Guindon, L.; Kimes, D.S. Regional aboveground forest biomass using airborne and spaceborne LiDAR in Québec. *Remote Sens. Environ.* **2008**, *112*, 3876–3890. [CrossRef]
35. García, M.; Saatchi, S.; Ustin, S.; Balzter, H. Modelling forest canopy height by integrating airborne LiDAR samples with satellite Radar and multispectral imagery. *Int. J. Appl. Earth Obs. Geoinf.* **2018**, *66*, 159–173. [CrossRef]
36. Bolton, D.K.; White, J.C.; Wulder, M.A.; Coops, N.C.; Hermosilla, T.; Yuan, X. Updating stand-level forest inventories using airborne laser scanning and Landsat time series data. *Int. J. Appl. Earth Obs. Geoinf.* **2018**, *66*, 174–183. [CrossRef]
37. Jin, S.; Su, Y.; Gao, S.; Hu, T.; Liu, J.; Guo, Q. The transferability of Random Forest in canopy height estimation from multi-source remote sensing data. *Remote Sens.* **2018**, *10*, 1183. [CrossRef]
38. Zald, H.S.; Wulder, M.A.; White, J.C.; Hilker, T.; Hermosilla, T.; Hobart, G.W.; Coops, N.C. Integrating Landsat pixel composites and change metrics with lidar plots to predictively map forest structure and aboveground biomass in Saskatchewan, Canada. *Remote Sens. Environ.* **2016**, *176*, 188–201. [CrossRef]
39. Ferraz, A.; Saatchi, S.; Xu, L.; Hagen, S.; Chave, J.; Yu, Y.; Meyer, V.; Garcia, M.; Silva, C.; Roswintiart, O.; et al. Carbon storage potential in degraded forests of Kalimantan, Indonesia. *Environ. Res. Lett.* **2018**, *13*, 095001. [CrossRef]

40. Shao, Z.; Zhang, L.; Wang, L. Stacked sparse autoencoder modeling using the synergy of airborne LiDAR and satellite optical and SAR data to map forest above-ground biomass. *IEEE J. Sel. Top. Appl. Earth Obs. Remote Sens.* **2017**, *10*, 5569–5582. [CrossRef]
41. Wulder, M.A.; White, J.C.; Bater, C.W.; Coops, N.C.; Hopkinson, C.; Chen, G. Lidar plots—A new large-area data collection option: Context, concepts, and case study. *Can. J. Remote Sens.* **2012**, *38*, 600–618. [CrossRef]
42. Selangor State Forestry Department. *Integrated Management Plan for North Selangor Peat Swamp Forest 2014–2023*; Selangor State Forestry Department: Shah Alam, Malaysia, 2014.
43. Ahmed, N. *Guardians of the North Selangor Peat Swamp Forest*; Peatlands International: Québec, QC, Canada, 2014.
44. Tonks, A.J.; Aplin, P.; Beriro, D.J.; Cooper, H.; Evers, S.; Vane, C.H.; Sjögersten, S. Impacts of conversion of tropical peat swamp forest to oil palm plantation on peat organic chemistry, physical properties and carbon stocks. *Geoderma* **2017**, *289*, 36–45. [CrossRef]
45. Azhar, B.; Lindenmayer, D.B.; Wood, J.; Fischer, J.; Manning, A.; McElhinny, C.; Zakaria, M. The conservation value of oil palm plantation estates, smallholdings and logged peat swamp forest for birds. *For. Ecol. Manag.* **2011**, *262*, 2306–2315. [CrossRef]
46. Yule, C.M. Loss of biodiversity and ecosystem functioning in Indo-Malayan peat swamp forests. *Biodivers. Conserv.* **2010**, *19*, 393–409. [CrossRef]
47. Prentice, C.; Aikanathan, S. *A Preliminary Faunal Assessment of the North Selangor Peat Swamp Forest*; Asian Wetland Bureau: Kuala Lumpur, Malaysia, 1989.
48. Charters, L.J.; Aplin, P.; Marston, C.G.; Padfield, R.; Rengasamy, N.; Bin Dahalan, M.P.; Evers, S. Peat swamp forest conservation withstands pervasive land conversion to oil palm plantation in North Selangor, Malaysia. *Int. J. Remote Sens.* **2019**, *40*, 7409–7438. [CrossRef]
49. Drusch, M.; Del Bello, U.; Carlier, S.; Colin, O.; Fernandez, V.; Gascon, F.; Hoersch, B.; Isola, C.; Laberinti, P.; Martimort, P.; et al. Sentinel-2: ESA's optical high-resolution mission for GMES operational services. *Remote Sens. Environ.* **2012**, *120*, 25–36. [CrossRef]
50. Galidaki, G.; Zianis, D.; Gitas, I.; Radoglou, K.; Karathanassi, V.; Tsakiri–Strati, M.; Woodhouse, I.; Mallinis, G. Vegetation biomass estimation with remote sensing: Focus on forest and other wooded land over the Mediterranean ecosystem. *Int. J. Remote Sens.* **2017**, *38*, 1940–1966. [CrossRef]
51. Timothy, D.; Onisimo, M.; Riyad, I. Quantifying aboveground biomass in African environments: A review of the trade-offs between sensor estimation accuracy and costs. *Trop. Ecol.* **2016**, *57*, 393–405.
52. Fernández-Manso, A.; Fernández-Manso, O.; Quintano, C. SENTINEL-2A red-edge spectral indices suitability for discriminating burn severity. *Int. J. Appl. Earth Obs. Geoinf.* **2016**, *50*, 170–175. [CrossRef]
53. Frampton, W.J.; Dash, J.; Watmough, G.; Milton, E.J. Evaluating the capabilities of Sentinel-2 for quantitative estimation of biophysical variables in vegetation. *ISPRS J. Photogramm. Remote Sens.* **2013**, *82*, 83–92. [CrossRef]
54. Hijmans, R.J. Raster: Geographic Data Analysis and Modeling. R Package Version 2.8-4. 2018. Available online: https://CRAN.R-project.org/package=raster (accessed on 19 December 2018).
55. Haralick, R.M.; Shanmugam, K.; Dinstein, I.H. Textural features for image classification. *IEEE Trans. Syst. Man Cybern.* **1973**, *6*, 610–621. [CrossRef]
56. Zvoleff, A. glcm: Calculate Textures from Grey-Level Co-Occurrence Matrices (GLCMs). R Package Version 1.6.1. 2016. Available online: https://CRAN.R-project.org/package=glcm (accessed on 19 December 2018).
57. Regional Centre for Forest Management and Ecosystem Management Services. *Report on The Management Inventory of the North Selangor Peat Swamp Forest*; Malaysian-DANCED Project on Sustainable Managment of Peat Swamp Forest; Project Document Number 25; Malaysia Office: Petaling Jaya, Malaysia, 2000.
58. Chave, J.; Réjou-Méchain, M.; Búrquez, A.; Chidumayo, E.; Colgan, M.S.; Delitti, W.B.; Duque, A.; Eid, T.; Fearnside, P.M.; Goodman, R.C.; et al. Improved allometric models to estimate the aboveground biomass of tropical trees. *Glob. Chang. Biol.* **2014**, *20*, 3177–3190. [CrossRef] [PubMed]
59. Feldpausch, T.R.; Lloyd, J.; Lewis, S.L.; Brienen, R.J.W.; Gloor, M.; Mendoza, A.M.; Lopez-Gonzalez, G.; Banin, L.; Abu Salim, K.; Affum-Baffoe, K.; et al. Tree height integrated into pantropical forest biomass estimates. *Biogeosciences* **2012**, *9*, 3381–3403. [CrossRef]
60. Chauve, A.; Bretar, F.; Durrieu, S.; Pierrot-Deseilligny, M.; Puech, W. Fullanalyze: A research tool for handling, processing and analyzing full-waveform LiDAR data. In Proceedings of the 2009 IEEE International Geoscience and Remote Sensing Symposium, Cape Town, South Africa, 12–17 July 2009; Volume 4, p. IV-841.
61. Zanne, A.E.; Lopez-Gonzalez, G.; Coomes, D.A.; Ilic, J.; Jansen, S.; Lewis, S.L.; Miller, R.B.; Swenson, N.G.; Wiemann, M.C.; Chave, J. Global Wood Density Database. Dryad Identifier. 2009. Available online: http://hdl.handle.net/10255/dryad.235 (accessed on 19 December 2018).
62. Réjou-Méchain, M.; Tanguy, A.; Piponiot, C.; Chave, J.; Hérault, B. biomass: An r package for estimating above-ground biomass and its uncertainty in tropical forests. *Methods Ecol. Evol.* **2017**, *8*, 1163–1167. [CrossRef]
63. Breiman, L. Random forests. *Mach. Learn.* **2001**, *45*, 5–32. [CrossRef]
64. Karlson, M.; Ostwald, M.; Reese, H.; Sanou, J.; Tankoano, B.; Mattsson, E. Mapping tree canopy cover and aboveground biomass in Sudano-Sahelian woodlands using Landsat 8 and random forest. *Remote Sens.* **2015**, *7*, 10017–10041. [CrossRef]
65. Main-Knorn, M.; Moisen, G.G.; Healey, S.P.; Keeton, W.S.; Freeman, E.A.; Hostert, P. Evaluating the remote sensing and inventory-based estimation of biomass in the Western Carpathians. *Remote Sens.* **2011**, *3*, 1427–1446. [CrossRef]

66. Curran, P.J.; Hay, A.M. The importance of measurement error for certain procedures in remote sensing at optical wavelengths. *Photogramm. Eng. Remote Sens.* **1986**, *52*, 229–241.
67. Wright, M.N.; Ziegler, A. ranger: A fast implementation of random forests for high dimensional data in C++ and R. *arXiv* **2015**, arXiv:1508.04409. [CrossRef]
68. Davies, J. Training Module on Peatland Assessment and Management. In *ASEAN Peatland Forests Project*; ASEAN Secretariat and Global Environment Centre: Kuala Lumpur, Malaysia, 2011.
69. Prentice, R.C. The Peatland Biodiversity Management Toolbox: A Handbook for the Conservation and Management of Peatland Biodiversity in Southeast Asia. In *A Compilation. ASEAN Peatland Forests Project–Rehabilitation and Sustainable Use of Peatland Forests in Southeast Asia*; ASEAN Secretariat and the Global Environment Centre: Kuala Lumpur, Malaysia, 2011.
70. Secretariat, A.S.E.A.N.; Global Environment Centre. *Peatlands in Southeast Asia–A Profile. Rehabilitation and Sustainable Use of Peatland Forests in Southeast Asia, ASEAN Peatland Forests Project*; ASEAN Secretariat: Jakarta, Indonesia, 2011.
71. Alam, M.J.; Rengasamy, N.; bin Dahalan, M.P.; Halim, S.A.; Nath, T.K. Socio-economic and ecological outcomes of a community-based restoration of peatland swamp forests in Peninsular Malaysia: A 5Rs approach. *Land Use Policy* **2022**, *122*, 106390. [CrossRef]
72. Cattau, M.E.; Harrison, M.E.; Shinyo, I.; Tungau, S.; Uriarte, M.; DeFries, R. Sources of anthropogenic fire ignitions on the peat-swamp landscape in Kalimantan, Indonesia. *Glob. Environ. Chang.* **2016**, *39*, 205–219. [CrossRef]
73. Page, S.; Hosciło, A.; Wösten, H.; Jauhiainen, J.; Silvius, M.; Rieley, J.; Ritzema, H.; Tansey, K.; Graham, L.; Vasander, H.; et al. Restoration ecology of lowland tropical peatlands in Southeast Asia: Current knowledge and future research directions. *Ecosystems* **2009**, *12*, 888–905. [CrossRef]
74. Dahalan, M.P.; Manaf, M.B.A.; Rahman, B.H.A.; Khalid, S.M.A.S.; Sukri, A.M.; Yusoff, D.M.; Muda, M. Implementation of Integrated Management Plan for North Selangor Peat Swamp Forest 2014–2023. In Proceedings of the 15th International Peat Congress, Sarawak, Malaysia, 15–19 August 2016; pp. 15–19.
75. Rengasamy, N.; Parish, F.; Lew, S.Y.; Azura, N. Peatland Rehabilitation Efforts in North Selangor Peat Swamp Forests. In Proceedings of the 15th International Peat Congress, Sarawak, Malaysia, 15–19 August 2016.
76. Wösten, J.H.M.; Rieley, J.O.; Page, S.E. *Restoration of Tropical Peatlands*; Alterra—Wageningen University and Research Centre, and the EU INCO—RESTORPEAT Partnership: Wageningen, The Netherlands, 2008; 252p, ISBN 978-90-327-0361-5.
77. Adam, E.; Mutanga, O.; Abdel-Rahman, E.M.; Ismail, R. Estimating standing biomass in papyrus (*Cyperus papyrus* L.) swamp: Exploratory of in situ hyperspectral indices and random forest regression. *Int. J. Remote Sens.* **2014**, *35*, 693–714. [CrossRef]
78. Lawrence, R.L.; Wood, S.D.; Sheley, R.L. Mapping invasive plants using hyperspectral imagery and Breiman Cutler classifications (RandomForest). *Remote Sens. Environ.* **2006**, *100*, 356–362. [CrossRef]
79. Chrysafis, I.; Mallinis, G.; Siachalou, S.; Patias, P. Assessing the relationships between growing stock volume and Sentinel-2 imagery in a Mediterranean forest ecosystem. *Remote Sens. Lett.* **2017**, *8*, 508–517. [CrossRef]
80. Laurin, G.V.; Puletti, N.; Hawthorne, W.; Liesenberg, V.; Corona, P.; Papale, D.; Chen, Q.; Valentini, R. Discrimination of tropical forest types, dominant species, and mapping of functional guilds by hyperspectral and simulated multispectral Sentinel-2 data. *Remote Sens. Environ.* **2016**, *176*, 163–176. [CrossRef]
81. Sarker, L.R.; Nichol, J.E. Improved forest biomass estimates using ALOS AVNIR-2 texture indices. *Remote Sens. Environ.* **2011**, *115*, 968–977. [CrossRef]
82. Cracknell, M.J.; Reading, A.M. Geological mapping using remote sensing data: A comparison of five machine learning algorithms, their response to variations in the spatial distribution of training data and the use of explicit spatial information. *Comput. Geosci.* **2014**, *63*, 22–33. [CrossRef]
83. Ham, J.; Chen, Y.; Crawford, M.M.; Ghosh, J. Investigation of the random forest framework for classification of hyperspectral data. *IEEE Trans. Geosci. Remote Sens.* **2005**, *43*, 492–501. [CrossRef]
84. Pettorelli, N.; Laurance, W.F.; O'Brien, T.G.; Wegmann, M.; Nagendra, H.; Turner, W. Satellite remote sensing for applied ecologists: Opportunities and challenges. *J. Appl. Ecol.* **2014**, *51*, 839–848. [CrossRef]
85. Nagendra, H.; Lucas, R.; Honrado, J.P.; Jongman, R.H.; Tarantino, C.; Adamo, M.; Mairota, P. Remote sensing for conservation monitoring: Assessing protected areas, habitat extent, habitat condition, species diversity, and threats. *Ecol. Indic.* **2013**, *33*, 45–59. [CrossRef]
86. Panta, M.; Kim, K.; Joshi, C. Temporal mapping of deforestation and forest degradation in Nepal: Applications to forest conservation. *For. Ecol. Manag.* **2008**, *256*, 1587–1595. [CrossRef]
87. Kennedy, R.E.; Townsend, P.A.; Gross, J.E.; Cohen, W.B.; Bolstad, P.; Wang, Y.Q.; Adams, P. Remote sensing change detection tools for natural resource managers: Understanding concepts and tradeoffs in the design of landscape monitoring projects. *Remote Sens. Environ.* **2009**, *113*, 1382–1396. [CrossRef]
88. Willis, K.S. Remote sensing change detection for ecological monitoring in United States protected areas. *Biol. Conserv.* **2015**, *182*, 233–242. [CrossRef]
89. Kennedy, R.E.; Andréfouët, S.; Cohen, W.B.; Gómez, C.; Griffiths, P.; Hais, M.; Healey, S.P.; Helmer, E.H.; Hostert, P.; Lyons, M.B.; et al. Bringing an ecological view of change to Landsat-based remote sensing. *Front. Ecol. Environ.* **2014**, *12*, 339–346. [CrossRef] [PubMed]

90. Duncanson, L.; Armston, J.; Disney, M.; Avitabile, V.; Barbier, N.; Calders, K.; Carter, S.; Chave, J.; Herold, M.; Crowther, T.W.; et al. The importance of consistent global forest aboveground biomass product validation. *Surv. Geophys.* **2019**, *40*, 979–999. [CrossRef] [PubMed]
91. Butler, D. Many eyes on Earth: Swarms of small satellites set to deliver close to real-time imagery of swathes of the planet. *Nature* **2014**, *505*, 143–144. [CrossRef] [PubMed]
92. Sandau, R.; Brieß, K.; D'Errico, M. Small satellites for global coverage: Potential and limits. *ISPRS J. Photogramm. Remote Sens.* **2010**, *65*, 492–504. [CrossRef]
93. Hand, E. Startup liftoff. *Science* **2015**, *348*, 172. [CrossRef]
94. Gill, E.; Sundaramoorthy, P.; Bouwmeester, J.; Zandbergen, B.; Reinhard, R. Formation flying within a constellation of nano-satellites: The QB50 mission. *Acta Astronaut.* **2013**, *82*, 110–117. [CrossRef]
95. Safyan, M. Planet's dove satellite constellation. In *Handbook of Small Satellites: Technology, Design, Manufacture, Applications, Economics and Regulation*; Springer International Publishing: Cham, Switzerland, 2020; pp. 1057–1073.
96. Planet Labs. Tracking Forests Globally. High Quality, Accessible, and Consistent Data on Global Forest Change. 2024. Available online: https://www.planet.com/products/forest-carbon/ (accessed on 4 May 2024).

Disclaimer/Publisher's Note: The statements, opinions and data contained in all publications are solely those of the individual author(s) and contributor(s) and not of MDPI and/or the editor(s). MDPI and/or the editor(s) disclaim responsibility for any injury to people or property resulting from any ideas, methods, instructions or products referred to in the content.